analytical chemistry

pubs.acs.org/ac Article

Stressor-Actuated Proximity Labeling for Reporting Cellular Interaction

Guyu Wang, Yichun Wang, Lan Wang, Shijie Wu, Ao Cao, Wenyuan Pu, Tielei Li, Ran Xie, Hongwei Wang, Lin Ding,* and Huangxian Ju

Cite This: *Anal. Chem.* 2024, 96, 20065−20073 Read Online

ACCESS | Metrics & More | Article Recommendations | Supporting Information

ABSTRACT: Cell-cell interactions determine the activation state and function of cells. When host cells are exposed to stressors such as microorganisms, immune defense machinery is activated to release H_2O_2, providing direct evidence of the relevant cellular physiological processes. Inspired by the fact that peroxidase can catalyze proximity labeling in the presence of exogenous H_2O_2, a stressor-actuated proximity labeling (SAPL) strategy is developed to report the process information on cell−cell interactions by recording stress levels. The stressors are covalently modified with horseradish peroxidase (HRP) and the H_2O_2 released by the host cells in response to the stressors triggers HRP-based proximity labeling. Using a fungal mimic or live fungi as stressors, the stress levels of different host cells are compared by in situ imaging of the labeling signals. The ability to accumulate stress signals allows SAPL to more sensitively differentiate between interactions involving different macrophage phenotypes. SAPL is also a powerful tool for real-time, in situ monitoring of the effects of surface modifications on cellular interactions. Thus, the SAPL strategy represents a new perspective in the monitoring of cell−cell interactions using endogenous effector molecules.

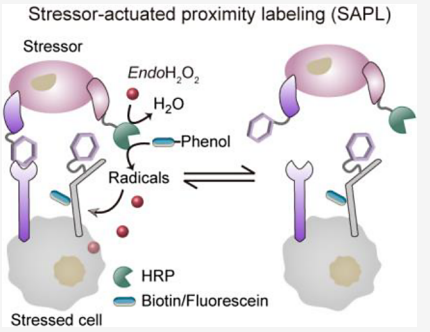

Cells transmit biological signals through direct contact or diffusive molecules, which causes changes in cellular states and dictates cellular functions.[1,2] Proximity labeling technologies, which have flourished in recent years, are capable of generating covalent labels at cellular interaction interfaces and thus serve as important tools for understanding intercellular communication at the molecular level.[3−14] The design principles generally involve the use of biological enzymes[3−11] or photocatalysts[12−14] mounted on "bait" cells to generate reactive intermediates from exogenous substrates or to remodel endogenous substrates to produce covalent markers on "prey" cells based on the proximity effect.

As a representative, peroxidase-based proximity labeling methods catalyze the generation of phenoxy radicals from phenol derivatives to label proximal amino acid sites (tyrosine, etc.) in the presence of exogenous hydrogen peroxide ($ExoH_2O_2$) (Figure 1).[3,4,15−18] These methods have the advantage of fast labeling speed (<1 min) and are widely adopted to study subcellular organelle proteomes[3,15,16] and cellular interactomics.[4,17] Underhill's group recently exploited peroxidase-expressed microorganisms to invade macrophages and perform proximity labeling in phagosomes, further expanding the application of this technique.[3] Due to the very short treatment time of H_2O_2, these technologies collect the "spatial proximity information" at the time of H_2O_2 addition. Moreover, the methods are only applicable to biosystems that are not sensitive to H_2O_2. This inspired us to consider using endogenous H_2O_2 to monitor the dynamic cellular interaction processes.

H_2O_2 is an important messenger molecule regulating several key signaling pathways and can accumulate intracellularly when cells are exposed to various stressors.[19−21] Peroxidases have been expressed intracellularly or immobilized on the cell surface to convert endogenous H_2O_2 into labels on proteins, indicating the location of H_2O_2 accumulation and unveiling the physiological functions of H_2O_2.[22−24] During immune defense, H_2O_2 is also released from cells to kill invading pathogens or directly regulate the activation states of immune cells.[25−27] Therefore, we envisioned that endogenous H_2O_2 released by the cellular stress during cell−cell interactions can be utilized to trigger proximity labeling, and the "interaction process information" can be reported by accumulating the stress signals.

We herein mounted horseradish peroxidase (HRP) on the stressors to develop a stressor-actuated proximity labeling (SAPL) strategy for reporting the cellular interaction. Endogenous H_2O_2 ($EndoH_2O_2$) released by the host cell in response to the stressor triggers HRP to catalyze the conversion of phenol derivatives to free radicals, which labels the proximal region of the interaction site (Figure 1). The cumulative labeling signals of H_2O_2 reflect the total stress level of host cells. Unlike

Received: September 16, 2024
Revised: November 23, 2024
Accepted: November 25, 2024
Published: December 2, 2024

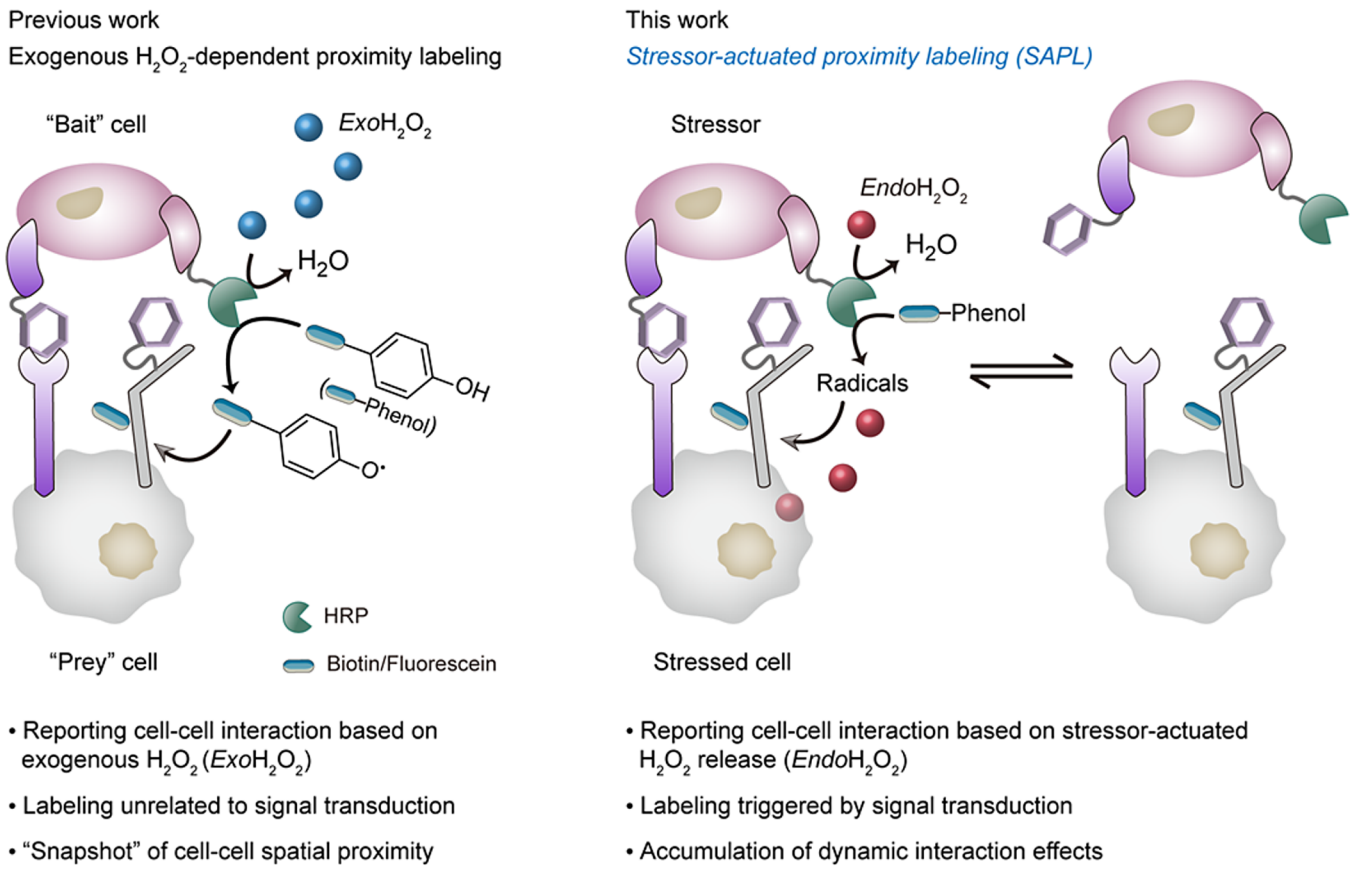

Figure 1. Schematic illustration of stressor-actuated proximity labeling (SAPL). In previous works, horseradish peroxidase (HRP)-based proximity labeling techniques rely on exogenous hydrogen peroxide (*Exo*H_2O_2) to trigger the catalysis of phenol derivatives to label proximal biomolecules for cell−cell interaction analysis. In contrast, the SAPL is actuated by endogenous H_2O_2 (*Endo*H_2O_2) released during the interaction, with the labeling signals reflecting the accumulated stress levels of cells in the interaction time window.

existing reporting technologies for cell−cell interactions, the strategy we developed reports interactions based on cumulative measurement of the "effects" of intrinsic cellular signal transduction, representing a novel perspective for evaluating interactions while providing spatial proximity information. Using a fungal mimic (zymosan)[28] and fungi (*Saccharomyces cerevisiae*) as stressors, we evaluated the differences in cellular stress levels using SAPL in both single and mixed-cell populations. We showed in situ that macrophages of the "M1" phenotype have higher stress levels than macrophages of the "M0" phenotype upon exposure to fungi invasion, and demonstrated that interactions can be more sensitively discriminated by recording the dynamic information reflected in the cumulative labeling signals. We further modified the surface of fungi with different polymers and achieved real-time monitoring of the effects of cell surface engineering on interactions using the SAPL platform. This work provides a powerful research tool with strong potential applications in cell surface engineering, adoptive cell therapy development, and tissue engineering.

EXPERIMENTAL SECTION

Preparation of Yeast@HRP. After one wash with PBS by centrifugation (860 × *g*, 2 min), the yeast was resuspended in an 800 μL PBS solution containing 500 μM NHS-PEG1000-biotin with an OD_{600} value of 1. The yeast suspension was placed in a rotary incubator for 2 h at room temperature, followed by washing (860 × *g*, 3 min) by centrifugation. The prepared biotin-modified yeast was then incubated in a 500 μL PBS solution containing 5 μg/mL SA-HRP in a rotary incubator for 30 min at room temperature. After two washes by centrifugation, Yeast@HRP were prepared. The yeast sample without treatment with NHS-PEG1000-biotin and SA-HRP was used as a control.

Performing SAPL on Macrophages Using Yeast@HRP. RAW264.7 macrophages of the "M1" phenotype were cultured in 35 mm diameter four-well dishes as described in "Immunofluorescence assay of macrophage phenotype" (Supporting Information).

Yeast@HRP samples were prepared with different concentrations of NHS-PEG1000-biotin and resuspended in DMEM. The final OD_{600} value was 0.6. Cells were subjected to incubation with a 100 μL Yeast@HRP suspension at 37 °C for 1 h, followed by two washes with PBS (Ca^{2+}, Mg^{2+}). The cells were then immersed in a 100 μL PBS (Ca^{2+}, Mg^{2+}) solution containing 10 μM FP for 1 h at 4 °C, followed by washing and the nuclear staining with Hoechst 33342 (2 μg/mL, 100 μL/well) for 30 min. Finally, CLSM imaging was performed (FP, ex: 495 nm, em: 505−600 nm; Hoechst 33342, ex: 405 nm, em: 420−480 nm). We defined the mean fluorescence intensity of the surface of a cell, after excluding the fluorescence signal of the adsorbed yeast, as the fluorescence signal (S) of that cell, with the fluorescence intensity of the surrounding cell-free regions as the background signal (B). We calculated the percentage of labeled cells in the total number of cells (100−500 cells) using

https://doi.org/10.1021/acs.analchem.4c05008
Anal. Chem. 2024, 96, 20065−20073

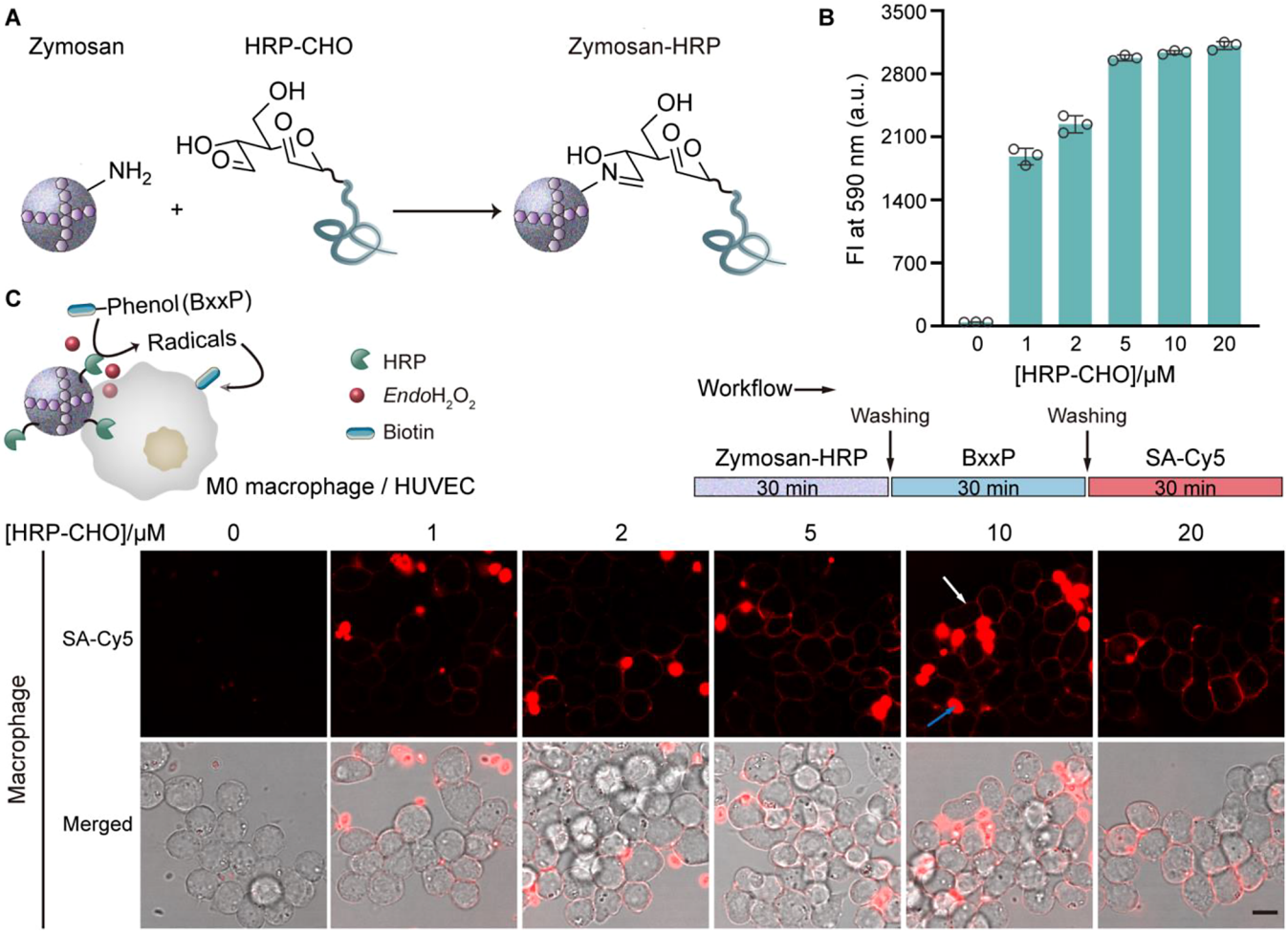

Figure 2. Zymosan-actuated proximity labeling on different cell types. (A) Schematic of the modification of HRP on zymosan. HRP-CHO was generated by the oxidation of glycans on HRP using sodium periodate and then reacted with the amino groups of zymosan, resulting in HRP-modified zymosan (Zymosan-HRP). (B) Characterization of the enzymatic activity in Zymosan-HRP using the HRP-catalyzed Amplex Red oxidation reaction, which generates resorufin with a maximum fluorescence emission at 590 nm. FI: fluorescence intensity. Data are shown as mean ± SD (n = 3). (C) CLSM imaging of zymosan-actuated proximity labeling on RAW264.7 macrophages. Biotin-XX tyramide (BxxP) was used as the labeling molecule, and stained with streptavidin-Cy5 (SA-Cy5). The white arrow indicates the signals on the macrophage; the blue arrow indicates the signals in zymosan. Scale bar: 10 μm. Data are representative of three independent experiments.

the signal-to-background (S/B) ratio greater than six as the threshold for cell labeling.

Yeast-Actuated Labeling on Macrophages of Different Phenotypes. RAW264.7 macrophages of the "M1" or "M0" phenotype (150 μL/well, 9×10^4 cells) were cultured in 35 mm diameter and four-well dishes as described in "Immunofluorescence assay of macrophage phenotype" (Supporting Information). Yeast@HRP (OD_{600} = 0.3, DMEM medium) was prepared with 500 μM NHS-PEG1000-biotin.

***Endo*H_2O_2 Group.** Cells were incubated with 100 μL Yeast@HRP for 1 h at 37 °C. After washing, 100 μL of PBS (Ca^{2+}, Mg^{2+}) solution containing 10 μM FP was added to the cells, and incubated for 30 min at 4 °C.

***Exo*H_2O_2 Group.** After incubation with Yeast@HRP and the subsequent washing, cells were treated with a 100 μL PBS (Ca^{2+}, Mg^{2+}) solution containing H_2O_2 (c_f = 1 mM) and FP (c_f = 10 μM) for 3 min at room temperature.

After FP labeling, cells in each group were stained with Hoechst 33342 and finally visualized by CLSM imaging.

SAPL on Macrophages of the "M0" Phenotype Using p(AAPBA)-Engineered Yeast. RAW264.7 macrophages of the "M0" phenotype (150 μL/well, 8×10^4 cells) were cultured for 1 day in 35 mm diameter four-well dishes.

After one wash by centrifugation (860 × g, 2 min), the yeast was resuspended in a 300 μL NHS-PEG1000-biotin solution (c_f = 500 μM) solution with an OD_{600} value of 1, followed by mixing with a 200 μL SA-HRP (c_f = 5 μg/mL). The prepared Yeast@HRP was then incubated with p(AEMA)-*b*-p(AAPBA) (c_f = 25 mg/mL, 200 μL, Figures S1−S6) in a rotary incubator at room temperature, followed by two washes. The product was resuspended in DMEM medium to prepare p(AAPBA)-engineered yeast (p(AAPBA)-Yeast@HRP).

Control groups:

1. Yeast@HRP: without p(AEMA)-*b*-p(AAPBA) modification.
2. p(AAPBA) (Fru) + Yeast@HRP: Fructose (c_f = 70 mM) and p(AEMA)-*b*-p(AAPBA) (c_f = 25 mg/mL) were mixed with a volume of 200 μL, and incubated in an incubator (800 rpm) at 25 °C for 1 h, followed by incubation with Yeast@HRP for 1 h.

Macrophages were treated with p(AAPBA)-Yeast@HRP and control yeast samples. The following procedures were

https://doi.org/10.1021/acs.analchem.4c05008
Anal. Chem. 2024, 96, 20065−20073

performed as described in "Yeast-Actuated Labeling on Macrophages of Different Phenotypes".

RESULTS AND DISCUSSION

Establishment of Stressor-Actuated Proximity Labeling (SAPL) Strategy. Zymosan is a particulate polysaccharide (4−5 μm in size) prepared from the cell wall of *Saccharomyces cerevisiae* and mainly composed of mannans, β-glucans, and proteins.[28] HRP is a typical glycoprotein, with glycan accounting for about 23% of the total molecular weight.[29] We prepared aldehyde-modified HRP (HRP-CHO) by oxidizing the glycans of HRP using sodium periodate.[29,30] HRP-mounted zymosan (Zymosan-HRP) was prepared by coupling amino groups on proteins in zymosan[28] with HRP-CHO to produce imine bonds (Schiff base) (Figure 2A,B).

It is reported that zymosan can stimulate various types of cells, including immune cells,[24,31] cancer cells,[32] and endothelial cells,[33] to release reactive oxygen species (ROS). We then used Zymosan-HRP as a fungal mimic stressor to invade RAW264.7 macrophages of the "M0" phenotype to test the feasibility of endogenous H_2O_2-triggered labeling (Figure 2C). The entire labeling process consisted of two steps: (1) incubation of cells with the stressor followed by removal of free Zymosan-HRP; (2) addition of biotin-modified tyramide (BxxP) to actuate the labeling process, which takes 30 min. The labeling signals on cell surfaces can be observed by fluorophore-modified streptavidin (SA-Cy5) staining. The Zymosan-HRP incubation resulted in distinct fluorescent signals, while without HRP modification, only a weak spot fluorescence could be observed (Figure 2C). There are two types of signal distribution patterns for the Zymosan-HRP group: (i) a linear fluorescent signal along the contour of the macrophage; and (ii) a strong spot fluorescence overlapping with the zymosan particle. These results indicate that the labeling depends on the HRP modification on zymosan. We then hypothesized that the binding of zymosan to the macrophage surface may trigger the release of endogenous H_2O_2, which activates HRP to catalyze the labeling of BxxP on the proximal macrophage surface (signal (i)) and zymosan (signal (ii)). The fluorescence signals on the macrophage surfaces reflect the cumulative "stress effect" of the dynamic interaction during the 30 min time window of labeling.

We also performed zymosan-actuated proximity labeling on human umbilical vein endothelial cells (HUVECs) (Figure S7). The extent of zymosan binding on HUVECs was not significantly different from that on macrophages, however, the labeling signals on the surfaces of HUVECs were weaker than those of macrophages. These data demonstrate the general applicability of SAPL for recording interactions using endogenous H_2O_2 and suggest that macrophages exhibit higher stress levels when exposed to the stressor zymosan.

Study of the Labeling Mechanism of SAPL. Next, we designed two groups of control experiments to explore the cause of the observed labeling signals on cells. The labeling signals were dramatically attenuated when catalase (an enzyme that can catalyze the decomposition of H_2O_2, 500 U/mL) was introduced into the BxxP labeling step, verifying endogenous H_2O_2-mediated cellular labeling (Figure S8).[24]

Considering that polysaccharides may compete with zymosan for glycan-binding sites on cells,[24] we used mannan and laminarin (β-glucan) to wash cells after coincubation of Zymosan-HRP and macrophages (or HUVECs), followed by BxxP labeling. The labeling signals on cells were significantly reduced when the concentration of each polysaccharide was 5 mg/mL, confirming that the glycan recognition-based affinity interaction between zymosan and cells mediates the labeling (Figure S9). These experiments demonstrate that stressor-

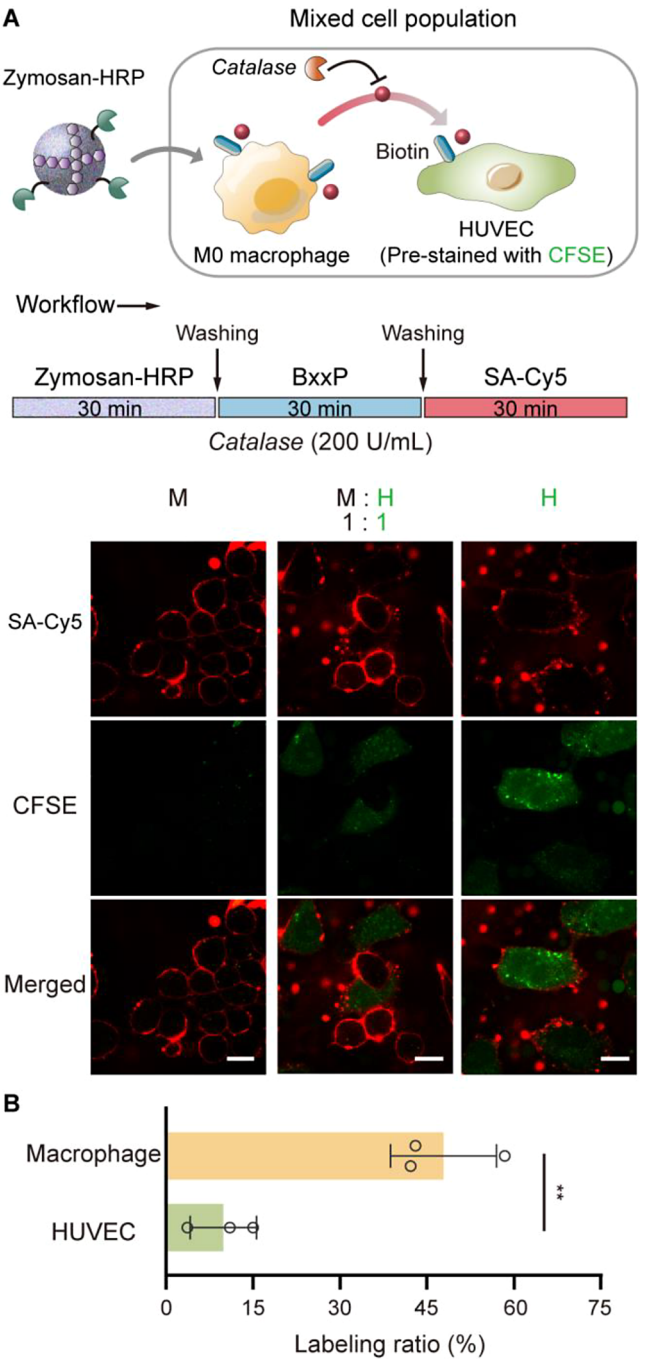

Figure 3. Zymosan-actuated proximity labeling in mixed cell populations. (A) Macrophages (M) and HUVECs (H, prestained with CFSE) were cocultured at a number ratio of 1:1. After Zymosan-HRP incubation, the BxxP labeling was performed in the presence of catalase (final concentration (c_f): 200 U/mL), followed by SA-Cy5 staining and CLSM imaging. Scale bars: 15 μm. Data are representative of three independent experiments. (B) Quantification of the cellular labeling ratios for the macrophage and HUVEC coculture group (1:1). A signal-to-background ratio greater than six was used as the threshold for cell labeling to calculate the number of labeled cells. The total number of cells ranged from 100 to 200. Data are shown as mean ± SD (n = 3). Statistical analysis was performed using the two-tailed unpaired t test. $^{**}P < 0.01$.

https://doi.org/10.1021/acs.analchem.4c05008
Anal. Chem. 2024, 96, 20065−20073

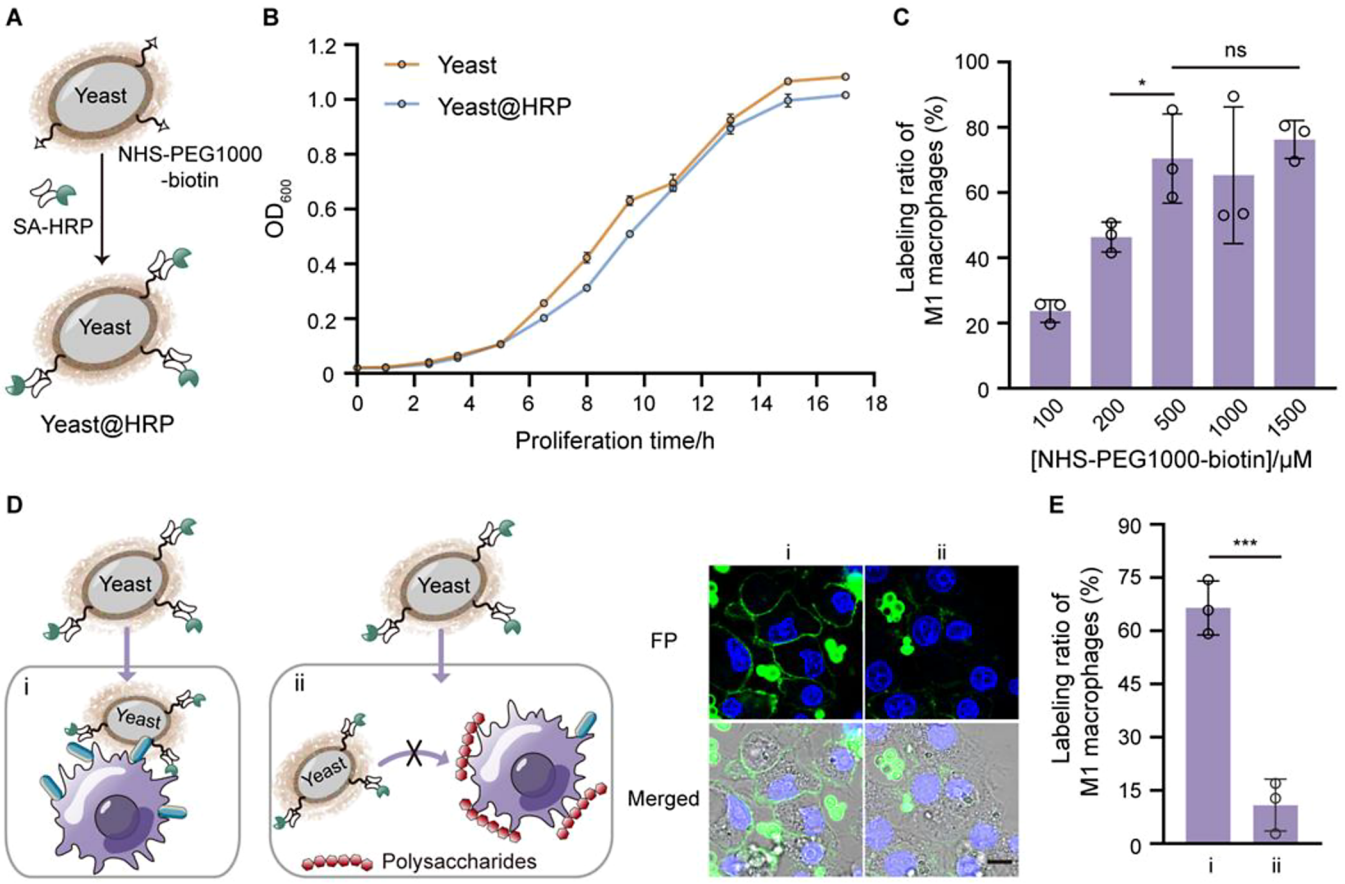

Figure 4. Yeast-actuated proximity labeling. (A) Schematic showing the preparation of Yeast@HRP. (B) Growth curves of yeast and Yeast@HRP. (C) The FP labeling ratio of "M1" macrophages actuated by Yeast@HRP. Yeast@HRP were prepared with different concentrations of NHS-PEG1000-biotin. (D) CLSM imaging of the labeling on macrophages under different treatment conditions. (i) Yeast@HRP-actuated cellular labeling; (ii) After Yeast@HRP incubation, macrophages were incubated with a polysaccharide (mannan and laminarin) solution, followed by direct FP labeling (without removal of excess polysaccharides). Scale bar: 10 μm. (E) Labeling ratio of macrophages in (D). In (B), (C), and (E), data are shown as mean ± SD (n = 3). Statistical analysis was performed using the two-tailed unpaired t test. *P < 0.05, ***P < 0.001, ns: not significant (P > 0.05). Data in (D) are representative of three independent experiments.

actuated labeling can indeed report the interactions between stressors and cells from the perspective of reflecting the stress level of cells.

In Situ Stress Level Assessment in Mixed Cell Populations. Since macrophages show higher stress levels than HUVECs when exposed to zymosan, we were interested in whether SAPL technology could be applied to assess cell stress levels in situ in mixed cell populations. Macrophages and HUVECs (prestained with CFSE dye) were mixed in a 1:1 number ratio and cocultured for 1 day, followed by incubation with Zymosan-HRP. To our surprise, the difference in labeling intensity between the two cell types was not obvious (Figure S10), perhaps due to diffusion of H_2O_2. To verify this, catalase (200 U/mL) was added during BxxP labeling to decompose intercellular diffusive H_2O_2. In this case, a higher fluorescence signal was observed on the macrophage than that on HUVECs (Figure 3A), the comparative trend of which was consistent with that in the case of separate culturing. The labeling ratio of macrophages was significantly higher than that of HUVECs in the cocultured system (Figure 3B), demonstrating that different levels of cell stress can be differentiated in the mixed cell system using SAPL.

Yeast-Actuated Host Cell Labeling. We then extended the SAPL platform to living fungi, using *Saccharomyces cerevisiae* (EBY100) as a model, to assess the microorganism-host cell interactions. The cell wall of *Saccharomyces cerevisiae* is mainly composed of mannosylated proteins, β-glucan, and chitin.[34] To improve the coupling efficiency and exposure degree of HRP, we utilized NHS-PEG1000-biotin as a linker to couple the yeast and streptavidin-HRP (SA-HRP) to yield Yeast@HRP (Figures 4A,B, and S11−S13).

Macrophages are characterized by phenotypic plasticity. Activated macrophages of the "M1" phenotype are involved in antimicrobial immunity[35,36] and were selected as the model cells to investigate the feasibility of yeast-actuated cell labeling. Lipopolysaccharide (LPS) and interferon-gamma (IFN-γ) were used to stimulate macrophages, and the "M1" phenotype was confirmed by immunofluorescence assay of CD86 (Figure S14).[37]

Macrophages were incubated with Yeast@HRP prepared with different concentrations of NHS-PEG1000-biotin, and fluorescein tyramide (FP) was used as the labeling molecule. As the concentration of NHS-PEG1000-biotin increased, the proportion of labeled macrophages in total macrophages gradually increased to a plateau, demonstrating that cell labeling depends on HRP catalysis and that the amount of HRP modification is a key factor in affecting *trans*-cellular labeling (Figures 4C and S15). When the cell labeling ratio reached the plateau, the concentration (500 μM) of NHS-PEG1000-biotin was consistent with the concentration at which the yeast surface reached

https://doi.org/10.1021/acs.analchem.4c05008
Anal. Chem. 2024, 96, 20065−20073

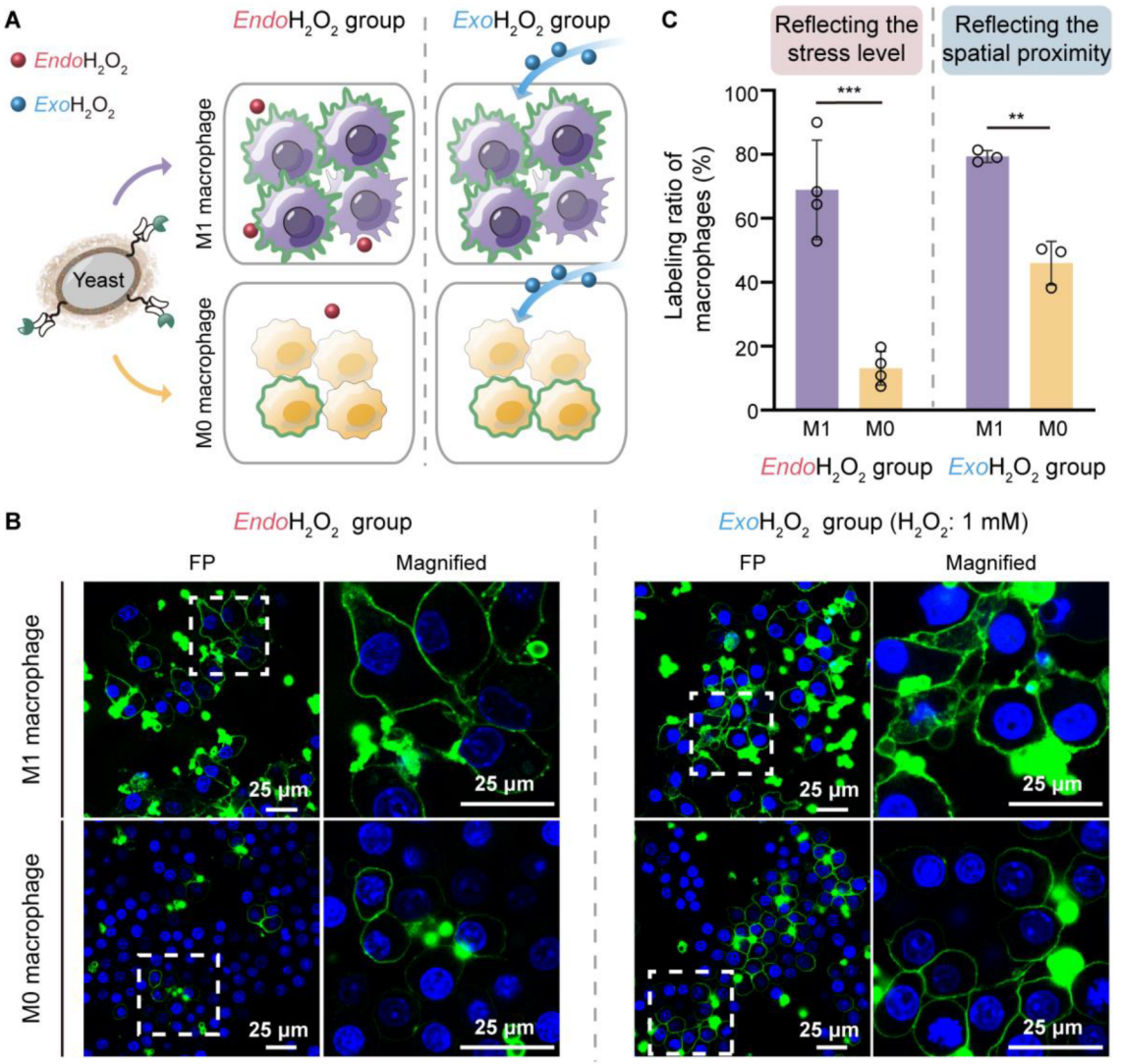

Figure 5. Assessment of the stress levels in macrophages of different phenotypes. Schematic (A) and CLSM imaging (B) of the FP labeling on macrophages actuated by Yeast@HRP (*Endo*H_2O_2 group) or in the presence of exogenous H_2O_2 (*Exo*H_2O_2 group). For the *Exo*H_2O_2 group, macrophages were subjected to Yeast@HRP incubation followed by FP treatment in the presence of 1 mM exogenous H_2O_2. Data are representative of four (*Endo*H_2O_2 group) and three (*Exo*H_2O_2 group) independent experiments. Scale bars: 25 μm. (C) Labeling ratio of macrophages in (B). Data are shown as mean ± SD ($n = 4$ for the *Endo*H_2O_2 group; $n = 3$ for the *Exo*H_2O_2 group). Statistical analysis was performed by the two-tailed unpaired *t* test. $^{**}P < 0.01$, $^{***}P < 0.001$.

saturation modification. This concentration was chosen for the subsequent experiments.

To verify the dependence of cell labeling on yeast-cell affinity interaction, after coincubation of Yeast@HRP and cells, polysaccharides (mannan and laminarin) were added to the cell mixture without subsequent washing, followed by FP labeling (Figure 4D). The labeling ratio of macrophages was dramatically reduced as a result of competition from polysaccharides (Figure 4E), demonstrating that the labeling signals originate from endogenous H_2O_2 release triggered by the glycan recognition-mediated interaction between the yeast and macrophages. We also achieved yeast-actuated labeling on HUVECs (Figure S16), proving the applicability of the method to different cell types.

Different Macrophage Phenotypes Show Different Stress Levels. The above experiments proved that SAPL can provide stress information on interactions by recording endogenous H_2O_2. Next, we were interested in whether macrophages of different phenotypes have different levels of stress during yeast invasion. We thus used Yeast@HRP as the stressor and FP as the labeling molecule and performed SAPL on both activated macrophages of the "M1" phenotype and resting macrophages of the "M0" phenotype (Figure 5A). There were more adhered yeast on "M1" macrophages than those on "M0" macrophages, and the cell labeling ratio of the "M1" phenotype was significantly higher (Figure 5B,C, *Endo*H_2O_2 group), demonstrating the capability of SAPL to discriminate different invasive interfaces. Using immunofluorescence staining, we confirmed that SAPL operation had little effect on CD86 expression in either macrophage type (Figure S17), suggesting that the macrophage phenotype was not altered by SAPL strategy.

To further highlight the feature of SAPL, we performed a control experiment in which H_2O_2 was added during FP labeling for a 3 min reaction (*Exo*H_2O_2 group). This group reflects the spatial proximity information on the cells at the time of H_2O_2 addition. The cell labeling ratios of the two phenotypes were different (Figure 5B,C, *Exo*H_2O_2 group), but the difference was

https://doi.org/10.1021/acs.analchem.4c05008
Anal. Chem. 2024, 96, 20065−20073

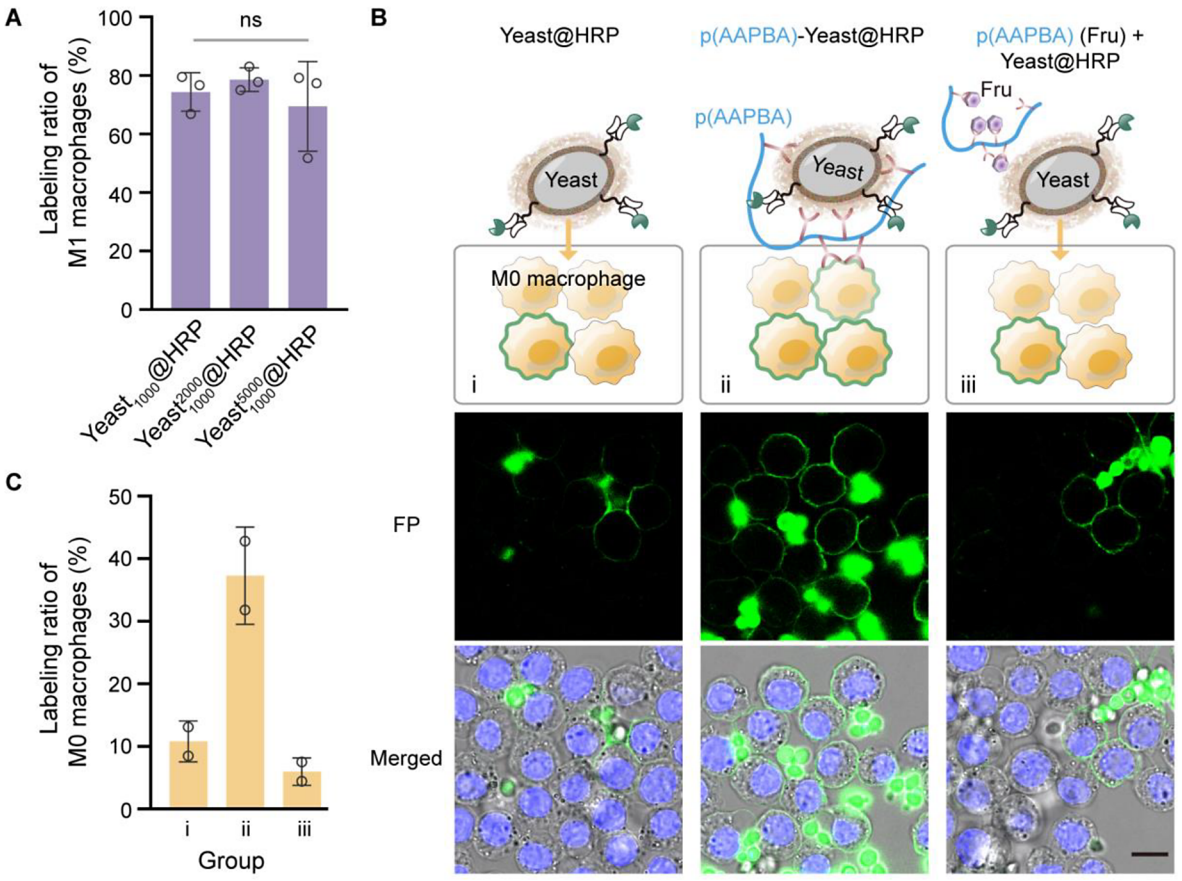

Figure 6. Monitoring of the effect of yeast surface modification on yeast-macrophage interactions using SAPL. (A) Labeling ratio of "M1" macrophages after SAPL by PEGylated Yeast@HRP. Data are shown as mean ± SD (n = 3), and the statistical analysis was performed using the ordinary One-way ANOVA with Tukey's multiple comparisons test. ns: not significant (P > 0.05). (B) Enhancement of yeast-macrophage interactions by coating yeast with p(AAPBA). (i) CLSM imaging of "M0" macrophages after SAPL by Yeast@HRP; (ii) CLSM imaging of "M0" macrophages after SAPL by p(AAPBA)-engineered yeast (p(AAPBA)-Yeast@HRP); (iii) a control experiment for (ii). Before SAPL, fructose-pretreated p(AAPBA) was used to coat Yeast@HRP to produce "p(AAPBA) (Fru) + Yeast@HRP" for incubation with "M0" macrophages. Data are representative of two independent experiments. Scale bar: 10 μm. (C) Labeling ratio in (B). Data are shown as mean ± SD (n = 2).

not as pronounced as in the *Endo*H_2O_2 group. We hypothesize that the more significant difference in the *Endo*H_2O_2 group is due to the ability of the SAPL technique to accumulate dynamic interaction "effects". During the 30 min time window of SAPL labeling, yeast and macrophages underwent a dynamic binding-dissociation process, as evidenced by the fact that there was less yeast adhering to "M0" macrophages than in the *Exo*H_2O_2 group. The temporary separation between cells may be reflected in the SAPL signals, allowing a more sensitive differentiation of interaction processes. Currently, the most typical means to evaluate macrophage phenotypes is the detection of biomarkers,[37−40] whereas our approach accomplishes this task by monitoring cellular stress levels.

Real-Time Stress Recording Reveals the Influence of Surface Engineering on Interactions. The regulation of cell−cell interactions through biological surface modification offers inspiring development opportunities in the field of biomedical engineering.[41−45] We sought to investigate the effect of PEG modification on yeast-macrophage interactions using the SAPL platform. To covalently modify yeast with PEG, we used active ester-modified PEG (NHS-PEG, including NHS-PEG2000-OH or NHS-PEG5000-OH) to couple with the amino groups of the cell wall, and prepared three types of modified yeast, designated as $Yeast^{2000}_{1000}$, $Yeast^{5000}_{1000}$, and $Yeast_{1000}$, respectively, wherein the subscript denotes NHS-PEG1000-biotin (for binding SA-HRP), and the superscript denotes NHS-PEG2000-OH or NHS-PEG5000-OH (for assessing the influence of PEG on yeast-"M1" macrophage interaction).

We constructed $Yeast_{1000}$@HRP, $Yeast^{2000}_{1000}$@HRP, and $Yeast^{5000}_{1000}$@HRP for invading "M1" macrophages and performing SAPL with FP as the labeling molecule (Figures 6A, S18, and S19). The modification of PEG2000 or PEG5000 had little effect on the stress level generated by the yeast invasion of macrophages. This result suggests that under these PEG length and density conditions, it is possible to simultaneously achieve yeast surface modification and avoid interfering with surface recognition.

Considering the dense glycan layer covering the yeast surface,[34] we then sought to regulate the interaction between yeast and macrophages by intervening glycan recognition. Phenylboronic acid (PBA) can react with *cis*-diols in saccharides, producing boronic esters.[46] Thus, we envisioned that PBA-functionalized polymers could serve as an "engager" to bridge yeast and macrophages, reinforcing their interaction. We selected macrophages of the "M0" phenotype as the model cells because these cells have lower stress levels upon Yeast@HRP invasion (Figure 5B,C).

https://doi.org/10.1021/acs.analchem.4c05008
Anal. Chem. 2024, 96, 20065−20073

We used the monomers 2-aminoethyl methacrylate (AEMA), 3-acrylamidophenylboronic acid (AAPBA), and tetraethylene glycol monomethacrylate (HEO_4MA) to synthesize the polymer p(AEMA)-*b*-p(AAPBA) (Figures S1−S6 and S20).[47] Yeast@HRP was incubated with p(AEMA)-*b*-p(AAPBA) for 1 h to allow p(AAPBA) to bind glycans on the yeast surface and prepare p(AAPBA)-Yeast@HRP. We also pretreated p(AEMA)-*b*-p(AAPBA) with fructose (Fru, 70 mM) for 1 h to block PBA moieties in the polymer and used this complex to incubate with Yeast@HRP to generate a control probe system "p(AAPBA) (Fru) + Yeast@HRP" to illustrate the action mechanism of p(AAPBA) (Figure 6B).

We performed SAPL by using Yeast@HRP after different treatments to invade "M0" macrophages. Compared to Yeast@HRP, the "p(AAPBA)-Yeast@HRP" group showed a significantly higher cell labeling ratio (ii versus i in Figure 6B,C), and more yeast were observed adhering to "M0" macrophages, suggesting that the "engager" enhanced cell−cell interaction. For the "p(AAPBA) (Fru) + Yeast@HRP" group, the cell labeling ratio decreased to the level of the Yeast@HRP group (iii versus i in Figure 6B,C), suggesting that p(AAPBA) bridges yeast and macrophages through glycan binding. These data confirm the real-time monitoring ability of SAPL to reveal the effect of surface engineering on cell−cell interactions. In addition, the "engager" may have the potential for microorganism-based cancer therapy and microbial colonization in the intestine.

CONCLUSIONS

We constructed a stressor-actuated proximity labeling platform at the interaction interface between the stressor and the host cell by mounting HRP on the stressor (zymosan or yeast).

The release of endogenous H_2O_2 actuated by stressors, can activate HRP to perform *cis*-labeling on the stressor and *trans*-labeling on the host cell. The *cis*-labeling signals reflect the adhesion states at the end of labeling, while the *trans*-labeling signals represent the cumulative stress effect. Unlike conventional HRP-catalyzed proximity labeling, it is an entirely new labeling platform to report the *process information* of the interaction from an *effect* perspective. We used SAPL to reveal the differences in the stress levels of macrophages of different phenotypes and found that the interactions could be more sensitively differentiated using SAPL compared to the exogenous H_2O_2-mediated proximity labeling method. We also monitored the effect of cell surface engineering on cell−cell interactions in real time. In the future, we will explore the following aspects: (1) applying the SAPL technology to more complex biological samples (e.g., blood samples) and scenarios (in vivo) to report the physiological states of host cells (e.g., inflammatory response); (2) identifying new targets regulating the interactions using the covalent labels produced by HRP-modified microorganisms on host cells and proteomics technologies.

ASSOCIATED CONTENT

Supporting Information

The Supporting Information is available free of charge at https://pubs.acs.org/doi/10.1021/acs.analchem.4c05008.

Experimental materials, reagents, apparatus, methods, ^1H NMR spectra for all compounds, supplementary figures, and the reference (PDF)

AUTHOR INFORMATION

Corresponding Author

Lin Ding − *State Key Laboratory of Analytical Chemistry for Life Science, School of Chemistry and Chemical Engineering and Chemistry and Biomedicine Innovation Center (ChemBIC), Nanjing University, Nanjing 210023, China;* orcid.org/0000-0001-5381-3484; Email: dinglin@nju.edu.cn

Authors

Guyu Wang − *State Key Laboratory of Analytical Chemistry for Life Science, School of Chemistry and Chemical Engineering, Nanjing University, Nanjing 210023, China*

Yichun Wang − *State Key Laboratory of Analytical Chemistry for Life Science, School of Chemistry and Chemical Engineering, Nanjing University, Nanjing 210023, China*

Lan Wang − *State Key Laboratory of Analytical Chemistry for Life Science, School of Chemistry and Chemical Engineering, Nanjing University, Nanjing 210023, China*

Shijie Wu − *State Key Laboratory of Coordination Chemistry, School of Chemistry and Chemical Engineering, Nanjing University, Nanjing 210023, China*

Ao Cao − *State Key Laboratory of Analytical Chemistry for Life Science, School of Chemistry and Chemical Engineering, Nanjing University, Nanjing 210023, China*

Wenyuan Pu − *Jiangsu Key Laboratory of Molecular Medicine, Medical School, Nanjing University, Nanjing 210093, China*

Tielei Li − *State Key Laboratory of Coordination Chemistry, School of Chemistry and Chemical Engineering and Department of Polymer Science & Engineering, School of Chemistry and Chemical Engineering, Nanjing University, Nanjing 210023, China*

Ran Xie − *State Key Laboratory of Coordination Chemistry, School of Chemistry and Chemical Engineering and Chemistry and Biomedicine Innovation Center (ChemBIC), Nanjing University, Nanjing 210023, China;* orcid.org/0000-0001-5170-2940

Hongwei Wang − *State Key Laboratory of Analytical Chemistry for Life Science, School of Chemistry and Chemical Engineering, Nanjing University, Nanjing 210023, China; Jiangsu Key Laboratory of Molecular Medicine, Medical School, Nanjing University, Nanjing 210093, China*

Huangxian Ju − *State Key Laboratory of Analytical Chemistry for Life Science, School of Chemistry and Chemical Engineering, Nanjing University, Nanjing 210023, China;* orcid.org/0000-0002-6741-5302

Complete contact information is available at: https://pubs.acs.org/10.1021/acs.analchem.4c05008

Author Contributions

All authors have given approval to the final version of the manuscript.

Notes

The authors declare no competing financial interest.

ACKNOWLEDGMENTS

We gratefully acknowledge support from the National Natural Science Foundation of China (22274073).

REFERENCES

(1) Bechtel, T. J.; Reyes-Robles, T.; Fadeyi, O. O.; Oslund, R. C. *Nat. Chem. Biol.* **2021**, *17*, 641−652.

(2) Belardi, B.; Son, S.; Felce, J. H.; Dustin, M. L.; Fletcher, D. A. *Nat. Rev. Mol. Cell Biol.* **2020**, *21*, 750−764.
(3) Li, K.; Chatterjee, A.; Qian, C.; Lagree, K.; Wang, Y.; Becker, C. A.; Freeman, M. R.; Murali, R.; Yang, W.; Underhill, D. M. *Nature* **2024**, *630*, 736−743.
(4) Martell, J. D.; Yamagata, M.; Deerinck, T. J.; Phan, S.; Kwa, C. G.; Ellisman, M. H.; Sanes, J. R.; Ting, A. Y. *Nat. Biotechnol.* **2016**, *34*, 774−780.
(5) Pasqual, G.; Chudnovskiy, A.; Tas, J. M. J.; Agudelo, M.; Schweitzer, L. D.; Cui, A.; Hacohen, N.; Victora, G. D. *Nature* **2018**, *553*, 496−500.
(6) Ge, Y.; Chen, L.; Liu, S.; Zhao, J.; Zhang, H.; Chen, P. R. *J. Am. Chem. Soc.* **2019**, *141*, 1833−1837.
(7) Liang, C.; He, J.; Zhao, X.; Hong, J.; Ma, X.; Mao, M.; Nie, W.; Wu, G.; Dong, Y.; Xu, W.; Huang, L.; Xie, H.-Y. *Angew. Chem., Int. Ed.* **2023**, *62*, No. e202304838.
(8) Liu, Q.; Zheng, J.; Sun, W. P.; Huo, Y. B.; Zhang, L. Y.; Hao, P. L.; Wang, H. P.; Zhuang, M. *Nat. Methods* **2018**, *15*, 715−722.
(9) Zhang, X.; Tang, Q.; Sun, J.; Guo, Y.; Zhang, S.; Liang, S.; Dai, P.; Chen, X. *Sci. Adv.* **2023**, *9*, No. eadg6388.
(10) Liu, Z. L.; Li, J. P.; Chen, M. K.; Wu, M. Y.; Shi, Y. J.; Li, W.; Teijaro, J. R.; Wu, P. *Cell* **2020**, *183*, 1117−1133.
(11) Yao, Y.; Jia, R.; Liu, C.; Wang, H.; Li, T.; Zheng, X.; Zhong, T.; Feng, N.; Sun, J.; Li, K.; Xie, R.; Ding, L.; Yan, C.; Ding, L.; Ju, H. *Angew. Chem., Int. Ed.* **2024**, *63*, No. e202407109.
(12) Oslund, R. C.; Reyes-Robles, T.; White, C. H.; Tomlinson, J. H.; Crotty, K. A.; Bowman, E. P.; Chang, D.; Peterson, V. M.; Li, L.; Frutos, S.; Vila-Perelló, M.; Vlerick, D.; Cromie, K.; Perlman, D. H.; Ingale, S.; OHara, S. D.; Roberts, L. R.; Piizzi, G.; Hett, E. C.; Hazuda, D. J.; Fadeyi, O. O. *Nat. Chem. Biol.* **2022**, *18*, 850−858.
(13) Qiu, S.; Li, W.; Deng, T.; Bi, A.; Yang, Y.; Jiang, X.; Li, J. P. *Angew. Chem., Int. Ed.* **2023**, *62*, No. e202303014.
(14) Zhang, Y.; Liu, S.; Guo, F.; Qin, S.; Zhou, N.; Liu, Z.; Fan, X.; Chen, P. R. *J. Am. Chem. Soc.* **2024**, *146*, 15186−15197.
(15) Rhee, H.-W.; Zou, P.; Udeshi, N. D.; Martell, J. D.; Mootha, V. K.; Carr, S. A.; Ting, A. Y. *Science* **2013**, *339*, 1328−1331.
(16) Lam, S. S.; Martell, J. D.; Kamer, K. J.; Deerinck, T. J.; Ellisman, M. H.; Mootha, V. K.; Ting, A. Y. *Nat. Methods* **2015**, *12*, 51−54.
(17) Loh, K. H.; Stawski, P. S.; Draycott, A. S.; Udeshi, N. D.; Lehrman, E. K.; Wilton, D. K.; Svinkina, T.; Deerinck, T. J.; Ellisman, M. H.; Stevens, B.; Carr, S. A.; Ting, A. Y. *Cell* **2016**, *166*, 1295−1307.
(18) Li, J.; Han, S.; Li, H.; Udeshi, N. D.; Svinkina, T.; Mani, D. R.; Xu, C.; Guajardo, R.; Xie, Q.; Li, T.; Luginbuhl, D. J.; Wu, B.; McLaughlin, C. N.; Xie, A.; Kaewsapsak, P.; Quake, S. R.; Carr, S. A.; Ting, A. Y.; Luo, L. *Cell* **2020**, *180*, 373−386.
(19) Sies, H.; Jones, D. P. *Nat. Rev. Mol. Cell Biol.* **2020**, *21*, 363−383.
(20) Sies, H.; Belousov, V. V.; Chandel, N. S.; Davies, M. J.; Jones, D. P.; Mann, G. E.; Murphy, M. P.; Yamamoto, M.; Winterbourn, C. *Nat. Rev. Mol. Cell Biol.* **2022**, *23*, 499−515.
(21) Sies, H.; Mailloux, R. J.; Jakob, U. *Nat. Rev. Mol. Cell Biol.* **2024**, *25*, 701−719.
(22) Kisty, E. A.; Falco, J. A.; Weerapana, E. *Cell Chem. Biol.* **2023**, *30*, 321−336.
(23) Mishra, P. K.; Park, I.; Sharma, N.; Yoo, C.-M.; Lee, H. Y.; Rhee, H.-W. *Anal. Chem.* **2022**, *94*, 14869−14877.
(24) Wang, G.; Li, Q.; Guo, Y.; Chen, L.; Yao, Y.; Zhong, Y.; Sun, J.; Yan, X.; Wang, H.; Wang, X.; Ding, L.; Ju, H. *Anal. Chem.* **2023**, *95*, 17798−17807.
(25) Ghezzi, P.; Rubartelli, A. *Curr. Opin. Chem. Biol.* **2023**, *76*, No. 102339.
(26) Nathan, C.; Cunningham-Bussel, A. *Nat. Rev. Immunol.* **2013**, *13*, 349−361.
(27) Reth, M. *Nat. Immunol.* **2002**, *3*, 1129−1134.
(28) Dicarlo, F. J.; Fiore, J. V. *Science* **1958**, *127*, 756−757.
(29) Cho, K. F.; Branon, T. C.; Udeshi, N. D.; Myers, S. A.; Carr, S. A.; Ting, A. Y. *Nat. Protoc.* **2020**, *15*, 3971−3999.
(30) Palaniappan, K. K.; Bertozzi, C. R. *Chem. Rev.* **2016**, *116*, 14277−14306.
(31) Makni-Maalej, K.; Chiandotto, M.; Hurtado-Nedelec, M.; Bedouhene, S.; Gougerot-Pocidalo, M.-A.; Dang, P. M.-C.; El-Benna, J. *Biochem. Pharmacol.* **2013**, *85*, 92−100.
(32) Ma, X.; Hu, W.; Guo, C.; Yu, L.; Gao, L.; Xie, J.; Li, C. *Adv. Funct. Mater.* **2014**, *24*, 5897−5903.
(33) Zhao, X.; Peng, M.; Wang, J.; Chen, S.; Lin, Y. *Analyst* **2022**, *147*, 4055−4062.
(34) Cow, N. A. R.; Lenardon, M. D. *Nat. Rev. Microbiol.* **2023**, *21*, 248−259.
(35) Chen, S. Z.; Saeed, A.; Liu, Q.; Jiang, Q.; Xu, H. Z.; Xiao, G. G.; Rao, L.; Duo, Y. H. *Signal Transduction Targeted Ther.* **2023**, *8*, 207.
(36) Murray, P. J.; Wynn, T. A. *Nat. Rev. Immunol.* **2011**, *11*, 723−737.
(37) Li, P.; Hao, Z.; Wu, J.; Ma, C.; Xu, Y.; Li, J.; Lan, R.; Zhu, B.; Ren, P.; Fan, D.; Sun, S. *Front. Immunol.* **2021**, *12*, No. 700009.
(38) Jiao, S.; Li, C.; Guo, F.; Zhang, J.; Zhang, H.; Cao, Z.; Wang, W.; Bu, W.; Lin, M.; Lue, J.; Zhou, Z. *Nat. Commun.* **2023**, *14*, 6416.
(39) Nasra, S.; Shah, T.; Bhatt, M.; Chaudhari, R.; Bhatia, D.; Kumar, A. *ACS Appl. Bio Mater.* **2023**, *6*, 2886−2897.
(40) Simkin, J.; Gawriluk, T. R.; Gensel, J. C.; Seifert, A. W. *eLife* **2017**, *6*, No. e24623.
(41) June, C. H.; O'Connor, R. S.; Kawalekar, O. U.; Ghassemi, S.; Milone, M. C. *Science* **2018**, *359*, 1361−1365.
(42) Gong, N.; Han, X.; Xue, L.; El-Mayta, R.; Metzloff, A. E.; Billingsley, M. M.; Hamilton, A. G.; Mitchell, M. J. *Nat. Mater.* **2023**, *22*, 1571−1580.
(43) Lin, M.; Chen, Y.; Zhao, S.; Tang, R.; Nie, Z.; Xing, H. *Angew. Chem., Int. Ed.* **2022**, *61*, No. e202111647.
(44) Csizmar, C. M.; Petersburg, J. R.; Wagner, C. R. *Cell Chem. Biol.* **2018**, *25*, 931−940.
(45) Wang, Y.; Li, Z.; Mo, F.; Chen-Mayfield, T.-J.; Saini, A.; LaMere, A. M.; Hu, Q. *Chem. Soc. Rev.* **2023**, *52*, 1068−1102.
(46) Kawada, M.; Jo, H.; Medina, A. M.; Sim, S. *J. Am. Chem. Soc.* **2023**, *145*, 16210−16217.
(47) Xu, J.; Jung, K.; Atme, A.; Shanmugam, S.; Boyer, C. *J. Am. Chem. Soc.* **2014**, *136*, 5508−5519.

https://doi.org/10.1021/acs.analchem.4c05008
Anal. Chem. 2024, 96, 20065−20073